COMPUTATIONAL PROBLEMS OF ELECTRICAL ENGINEERING

Vol. 4, No. 1, 2014

InSb MICROCRYSTALS FOR SENSOR ELECTRONICS

Anatoliy Druzhynin[1], Ihor Ostrovskyi[1], Yuriy Khoverko[1], Ihor Khytruk[1],
Krzysztof Rogacki[2]
[1] Lviv Polytechnic National University, Lviv, Ukraine,
druzh@polynet.lviv.ua
[2] Institute of Low Temperatures and Structure Research of Polish Academy of Sciences, Wroclaw, Poland

Abstract. The processes of electron scattering on the short-range potential caused by interaction with polar and nonpolar optical phonons, piezoelectric and acoustic phonons, static strain centers and ionized impurities in n-InSb with the defect concentration of 3×10^{17} cm^{-3} are considered. The temperature dependences of electron mobility ranged between 4,2 K and 500 K are calculated. Based on the InSb whiskers, there was elaborated a highly sensitive Hall sensor operating in the wide range of temperatures between 4,2 K and 500 K and magnetic fields (up to 10 T) with a sensitivity of ~ 3,5 mV/T.

Key words: charge carrier scattering, the Hall effect, mobility, InSb microcrystals, sensor

1. Introduction

The investigation of physical properties of low-dimensional structures was focused on the creation of new functional materials with unique properties. One of the problems of the research in the field of energy saving and sensor electronics is the development of new high-performance thermoelectric materials with linear thermoresistive characteristics. These criteria are well satisfied by the filamentary micro- and nanocrystals. A small nanowire diameter provides effective phonon scattering by surface, accompanied by a significant decrease in thermal conductivity [1, 2]. Recently, the thermoelectric properties of the InSb nanowires, placed in an asbestos envelope have been investigated intensively [3]. In particular, their Seebeck coefficient was measured in the wide temperature range [4, 5]. It was shown that the temperature dependence of the Seebeck coefficient for heavily doped samples are well described by Luttinger fluid theory [4]. The measured value of the thermal conductivity of the InSb nanowires at low temperatures turned out to be by several orders of magnitude lower than the corresponding bulk samples [5]. However, the above mentioned works do not clear up the contribution of an asbestos shell to the nanowire properties. Besides, the localization of the nanowires in this shell is unknown that complicates the calculations, leads to poor result reproducibility and prevents the development of nanowire-based electronic devices. More attractive is the research into naturally grown InSb whiskers, which are widely used in magnetic sensors [6]. Clearly, the temperature dependence of the main parameters (conductivity, the Seebeck coefficient, the Hall constant) of the whiskers are mainly determined by the priority mechanisms of carrier scattering, as well as the presence of structural defects in the crystal. Thus, the purposes of this work are applying the short-range models to describe the processes of electron scattering on impurities and various types of defects in the crystal lattice for the doped InSb whiskers, comparing the results of theoretical calculations with the empirical data, and predicting the performances of the Hall sensors designed on their basis.

2. Theoretical fundametals

The electron scattering in indium antimonide was usually considered in relaxation time approximation or using the variational method. The common feature of these methods is the use of the long-range charge carrier scattering models for the description of the transport phenomena in this semiconductor. In these models, it is supposed that the charge carrier interacts either with the entire crystal (electron -phonon interaction) or with the defect potential of the impurity, the action radius of which is equal to ~$10 - 100a_0$ (a_0 is the lattice constant). However, such an assumption has the following contradictions: a) it contradicts the special relativity according to which the charge carrier would interact only with a neighbouring crystal region; b) it contradicts the atomistic hypothesis according to which the charge carrier interacts (and transfers the energy respectively) only with one atom but not simultaneously with many atoms which are situated in different points of space. For these contradictions to be eliminated, it is necessary to answer the following question – what object in the crystal absorbs the energy while scattering the charge carrier? It can be either an ionized (neutral) impurity atom or an atom oscillating in a lattice site. While scattering, none of these objects leave the boundaries of the elementary cell. Therefore, the short-range charge carrier scattering models in zinc-blende II-VI [7, 8] and in wurtzite III-V [9, 10] semiconductors were proposed. The carrier in the models was supposed to interact with the defect potential only within one elementary cell. Here the following physical reasons were used: while scattering, the electron interacts only with a neighboring crystal region (the short-range principle), after scattering over this region, the electron interacts with the next neighboring crystal region, etc. The aim of the present paper is the use of the short-range models to describe the electron scattering on the various crystal lattice defects in indium antimonide.

According to the short-range scattering models in a zinc-blende structure semiconductor, the carrier transition probability from state k to state k′ caused by interaction with polar optical (PO), nonpolar optical (NPO), piezooptic (POP) and piezoacoustic (PAC), acoustic (AC) phonons, static strain (SS) potential, ionized impurity (II) looks like [7,8]:

$$\begin{aligned} W_{PO}(\mathbf{k},\mathbf{k}') = {} & \frac{64\,\pi^7 \gamma_{PO}^{10} e^4}{225\,\varepsilon_0^2 a_0{}^4 G} \frac{M_{In}+M_{Sb}}{M_{In}\,M_{Sb}} \cdot \\ & \cdot \left\{ \frac{1}{\omega_{LO}} \left[N_{LO}\delta(\varepsilon'-\varepsilon-\hbar\omega_{LO}) + \right.\right. \\ & \left. + (N_{LO}+1)\delta(\varepsilon'-\varepsilon+\hbar\omega_{LO}) \right] + \\ & + \frac{2}{\omega_{TO}} \left[N_{LO}\delta(\varepsilon'-\varepsilon-\hbar\omega_{LO}) + \right. \\ & \left.\left. + (N_{LO}+1)\delta(\varepsilon'-\varepsilon+\hbar\omega_{LO}) \right] \right\} \end{aligned} \tag{1}$$

$$\begin{aligned} W_{NPO}(\mathbf{k},\mathbf{k}') = {} & \frac{\pi^3 E_{NPO}{}^2}{288\,a_0{}^2 G} \frac{M_{In}+M_{Sb}}{M_{In}\,M_{Sb}} \cdot \\ & \cdot \left\{ \frac{1}{\omega_{LO}} \left[N_{LO}\delta(\varepsilon'-\varepsilon-\hbar\omega_{LO}) + \right.\right. \\ & \left. + (N_{LO}+1)\delta(\varepsilon'-\varepsilon+\hbar\omega_{LO}) \right] + \\ & + \frac{2}{\omega_{TO}} \left[N_{LO}\delta(\varepsilon'-\varepsilon-\hbar\omega_{LO}) + \right. \\ & \left.\left. + (N_{LO}+1)\delta(\varepsilon'-\varepsilon+\hbar\omega_{LO}) \right] \right\} \end{aligned} \tag{2}$$

$$\begin{aligned} W_{POP}(\mathbf{k},\mathbf{k}') = {} & \left(\frac{32}{75}\right)^2 \frac{\pi^9 e^2 e_{14}^2\, \gamma_{PZ}^{10}}{\varepsilon_0{}^2 G} \frac{M_{In}+M_{Sb}}{M_{\mathrm{In}}\,M_{Sb}} \cdot \\ & \cdot \left\{ \frac{1}{\omega_{LO}} \left[N_{LO}\delta(\varepsilon'-\varepsilon-\hbar\omega_{LO}) + \right.\right. \\ & \left. + (N_{LO}+1)\delta(\varepsilon'-\varepsilon+\hbar\omega_{LO}) \right] + \\ & + \frac{2}{\omega_{TO}} \left[N_{LO}\delta(\varepsilon'-\varepsilon-\hbar\omega_{LO}) + \right. \\ & \left.\left. + (N_{LO}+1)\delta(\varepsilon'-\varepsilon+\hbar\omega_{LO}) \right] \right\} \end{aligned} \tag{3}$$

$$\begin{aligned} W_{PAC}(\mathbf{k},\mathbf{k}') = {} & \frac{128\,\pi^7\, e^2\, e_{14}^2\, a_0^2\, \gamma_{\mathrm{PZ}}^{10}\, k_B T}{225\,\varepsilon_0^2\, \hbar\, \mathrm{G}\left[M_{In} + M_{Sb}\right]} \cdot \\ & \cdot \left(\frac{1}{c_{LO}} + \frac{2}{c_{TO}} \right)^2 \delta\,(\varepsilon'-\varepsilon)\,; \end{aligned} \tag{4}$$

$$\begin{aligned} W_{AC}(\mathbf{k},\mathbf{k}') = {} & \frac{\pi^3 k_B T\;\, E_{AC}^2}{144\,\hbar\,\mathrm{G}\left[M_{In} + M_{Sb}\right]} \cdot \\ & \cdot \left(\frac{1}{c_{||}} + \frac{2}{c_{\perp}} \right)^2 \delta\,(\varepsilon'-\varepsilon); \end{aligned} \tag{5}$$

$$W_{II}(\mathbf{k},\mathbf{k}') = \frac{\pi\, e^4 Z_i^2\, N_{II}\, \gamma_{II}^4\, a_0^4}{2\,\varepsilon_0^2\,\hbar\, V} \delta\,(\varepsilon'-\varepsilon)\,; \tag{6}$$

$$\begin{aligned} W_{SS}(\mathbf{k},\mathbf{k}') = {} & \frac{2^5 3^4 \pi^3 C^2 a_0^6 e^2\, e_{14}{}^2 N_{SS}}{V \varepsilon_0{}^2 \hbar} \cdot \\ & \cdot \frac{1}{q^2} \delta(\varepsilon'-\varepsilon), \end{aligned} \tag{7}$$

where M_{In}, M_{Sb} are the atom masses; G is the number of unit cells in crystal volume; ε_0 represents the vacuum permittivity; e denotes the elementary charge; k_B is the Boltzmann constant; $\hbar$ stands for the Planck constant; N_{LO}, N_{TO} are the number of longitudinal (LO) and transverse (TO) phonons with the frequency ω_{LO} and ω_{TO} respectively; e_{14} is the component of a piezoelectric tensor; $c_{\|}$, $c_{\perp}$ represent the respective sound velocities; V is the crystal volume; N_{II}, N_{SS} denote the ionized impurities and strain centers concentration respectively; Z_i is the impurity charge in electroncharge units; E_{AC}, E_{NPO} are the acoustic and optical deformation potentials respectively (valence band); γ_{PO}, γ_{PZ}, γ_{II} stand for the fitting parameters determining the action radius of the short-range potential ($R = \gamma a_0$, $0 \le \gamma_{PO}, \gamma_{PZ} \le 0.86$, $0 \le \gamma_{II} \le 1$); $q = |\mathbf{k}' - \mathbf{k}|$; $C \approx 0.1$.

It should be noted that the strong power dependence of the parameters γ_{PO}, γ_{PZ}, γ_{II} sharply limits the choice opportunities of their numerical values.

The parameters of the indium antimonide used for the calculation are listed in Table 1.

The Fermi level was determined from the charge neutrality equation given below:

$$n - p = N_D\,, \tag{8}$$

where N_D is the value of donors concentration.

Table 1

InSb parameters used in calculations

Material parameter	Value, temperature dependence	References
Atom masses, kg	M_{In} = $=19.06597\times10^{-26}$ M_{Sb} = $= 20.21872\times10^{-26}$	
Lattice constant, m	a_0 = $= 6.47937\times10^{-10}$	[11]
Energy gap, eV	$E_g = 0.235-$ -0.27×10^{-3} $T^2/(T+106)$	[12]
Energy equivalent of matrix element, eV	$E_p = 23.2$	[13]
Spin-orbit splitting, eV	$\Delta=0.803$	[14]
Density, gm · cm^{-3}	$\rho_0 = 5.7746$	[15]
Sound velosity, m · s^{-1}	$c_{\parallel}=3.77\cdot10^3$, $c_{\perp}=2.29\cdot10^3$	[16]
Optical deformation potential, eV	$E_{NPO}=26.8$	[17]
Acoustic deformation potential, eV	$E_{AC}=9.5$	[18]
Optical phonon frequency, rad · s^{-1}	$\omega_{TO}=3{,}39\cdot10^{13}$ $\omega_{LO}=3{,}59\cdot10^{13}$	[19]
Piezoelectric tensor component, C · m^{-2}	$e_{14}=0.071$	[20]

The calculation of the conductivity tensor components was done on the basis of the formalism of a precise solution to the stationary Boltzmann equation [21]. Using this formalism, one can obtain the additional fitting parameter γ_{SS} N_{SS} (we put $\gamma_{SS} = 1$) for an SS-scattering mode.

3. Comparison of theoretical and experimental results

A comparison of the theoretical temperature dependences of the electron mobility was performed with the experimental data, obtained on the InSb whiskers grown by a chemical vapour deposition method in the bromide system. The whiskers were doped with Sn impurity to the concentration that corresponds to metal-insulator transition.

The temperature investigations were conducted in the temperature range between 4,2K and 300K in the magnetic fields up to 14T. The samples were cooled down to 4,2 K in a helium cryostat. A special inset with a bifilar winding heater was used to heat up the samples to the room temperature. The stabilized electric current ranged between 100 μA and 1 mA was used depending on the sample resistance generated by the Keithley 224 current source. The Keithley 2000 and Keithley 2010 digital voltmeters with simultaneous automatic registration via a parallel port of PC, were used to measure voltage at the samples' potential contacts, the output of the thermocouple and magnetic field sensor with the accuracy of up to 1×10^{-6} V as well as for the vizualization and saving the data arrays into files. The Bitter-magnet- based setup was used to study the effect of strong magnetic fields on the samples. The induction of the magnet was 14T, deflection time – 1,75 T/min and 3,5 T/min at the temperature of ≤ 4,2 K respectively.

The experimentally obtained temperature dependence of InSb whiskers resistance is shown in Fig. 1. As seen in Fig. 1, the R(T) dependency for the InSb whiskers doped to the concentration corresponding to MIT contains the minimum temperature of about 70 K which correlates with a maximum of mobility (see Fig. 2).

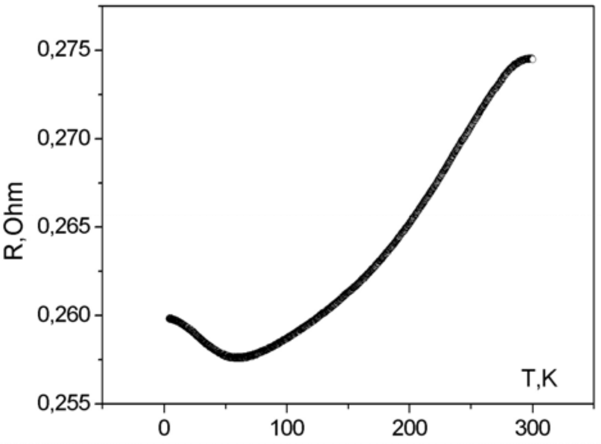

Fig. 1. Temperature dependence of InSb wires resistance.

The experimental dependence $\mu_n(T)$ for InSb whiskers is presented in Fig. 2. The solid lines represent the mobility calculated on the basis of the short-range models within the framework of the exact solution to the Boltzmann equation.

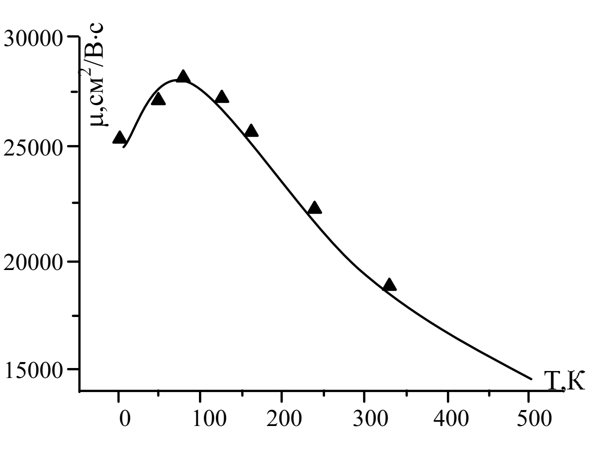

Fig. 2. Ttemperature dependence of electron mobility in InSb crystal with donor concentrations $N_D=3\times10^{17}cm^{-3}$.

The theoretical curves are seen to sufficiently agree with the experimental data in all the investigated temperature range. The obtained electron scattering parameters for different scattering modes are listed in Table 2.

Table 2

Parameters γ for different scattering modes

$N_{D,}$ (cm^{-3})	γ_{PO}	γ_{PZ}	γ_{II}	$\gamma_{SS}N_{SS}\times10^{-15}$ (cm^{-3})
3×10^{17}	0.60	0.45	0.30	13.7

To estimate the role of different scattering mechanisms, in Fig. 3, the dashed lines represent the appropriate dependences.

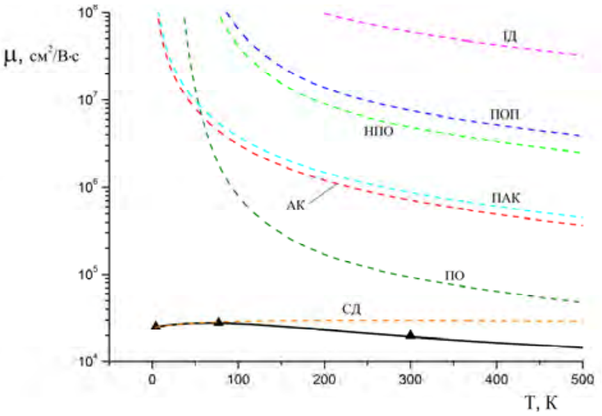

Fig. 3. Contribution of different scattering modes into electron mobility in InSb with donor concentrations $N_D=3\times10^{17}cm^{-3}$. The solid line is a mixed scattering mechanism.

In the whole temperature range, the main scattering mechanism is seen to be the static strain scattering. At higher temperatures, the contribution of the polar optical phonon scattering plays a dominant role. The other scattering mechanisms such as acoustic and piezo-acoustic phonon scattering, nonpolar and piezooptic phonon scattering, and ionized impurity scattering give negligibly small contributions.

4. Application of the results

Thus, the results of the calculations showed that the main mechanism of carrier scattering in InSb whiskers at low temperatures is the scattering by static strain. The source of this static strain is a crystal surface. When the whisker diameter becomes small, the effect of its surface causes the so-called Laplacian compression of sub-surface layers of the crystal. The effect of this natural strain is especially pronounced in the temperature dependences of the samples with a dopant concentration near the metal-insulator transition, in particular, can change the conductance from a metal to a semiconductor, as shown in the studied samples (Fig. 1). As a result, there is a weak temperature dependence of the resistivity in a wide temperature range between 4.2 K and 500 K, which is essential for the creation of sensors.

The Hall sensors are among a large number of physical quantities sensors [22] for wide application in aerospace engineering, cryogenic engineering, etc. Highly useful, high-speed, miniature sensors of physical quantities are efficient in difficult conditions, in different temperature ranges, i.e. at cryogenic temperatures.

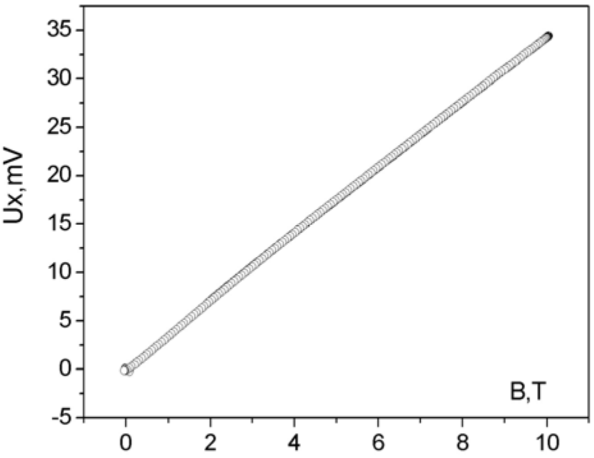

Fig. 4. Hall voltage versus magnetic field induction for InSb whiskers.

As shown by the experimental studies, the dependence of the Hall voltage on a magnetic field induction is linear (Fig. 4). Reproducibility of the signal across the field is high enough. This takes into account a weak temperature dependence of the resistivity within 1 % (see Fig.1). As a result, the field dependence of the Hall voltage is independent of the temperature ranged between 4,2 K and 500 K. On the other hand, the amplitude of the signal (35 mV) provides sufficient sensitivity to the measured parameter.

5. Conclusion

On the basis of the short-range principle, the electron scattering processes on various types of crystal defects in n-InSb have been considered. A sufficiently good agreement between the theory and experiment in the investigated temperature range has been established. Based on the research, a highly sensitive InSb Hall sensor has been elaborated. The sensor is able to function in a wide range of magnetic fields (up to 10 T) with a sensitivity of ~ 3,5 mV / T. The advantage of the sensors is stability of their performances in the wide temperature range between 4,2 K and 500 K.

References

[1] O. N. Uriupin, M. V. Vedernikov, A. A. Shabaldin, Y. V. Ivanov,Y. A. Kumzerov, and A. V. Fokin, “Thermoelectric properties of InSb nanowires over

a wide temperature range", *J. Electron. Mater.,* vol. 38, 990, 2009.

[2] A. I. Hochbaum, R. Chen, R. D. Delgado, W. Liang, E. C. Garnett, M. Najarian, A. Majumdar, and P. Yang, "Enhanced thermoelectric performance of rough silicon nanowires", *Nature*, vol. 451, no. 163, 2008.

[3] O. N. Uriupin, N. F. Kartenko, and N. Yu. Tabachkova, "Structure of InSb nanowires in chrysolite asbestos channels", *Fizika i tekhnika polyprovodnikov*, vol. 48, no. 7, pp. 1002–1006, 2014. (Russian)

[4] S. V. Zaitsev-Zotov, Yu. A. Kumzerov, Yu. A. Firsov, and P. Monceau, "Luttinger-liquid-like transport in long InSb nanowires", *J. Phys.: Condens. Matter,* vol. 12*,* no. 20, pp. L303-L309, 2000.

[5] Y. A. Kumzerov, A. V. Fokin, L. S. Parfenjeva, B. I. Smirnov, I. A. Smirnov, H. Misiorek, and A. Jezowski, "Thremoconductance and resistance of bulk nanostructured In in porous borosilica glass channels", *Fizika tverdogo tela*, vol. 55, no. 9, pp.1671–1676, 2013. (Russian)

[6] I. A. Bolshakova, R. L. Holyaka, O. Yu. Makido, and T. A. Marusenkova, "New condtructions of semiconductor 3-D sensors of magnetic field", *Elektronika i sviaz,* vol. 2–3, pp. 6–10, 2009. (Ukrainian)

[7] O. P. Malyk, "Electron scattering on the short-range potential in narrow gap $Cd_xHg_{1-x}Te$", *Mater. Sci. & Engineering B.,* vol. 129, pp. 161–171, 2006.

[8] O. P.Malyk, "The local electron interaction with crystal lattice defects in CdHgSe solid solution", *Phys. Status Solidi (c).*, vol. 6, pp.86–89, 2009.

[9] I.Gorczyca, "Scattering on Short-Range Potentials in InSb. A Pseudopotential Calculation", *Phys. Stat. Solidi (b).,* vol. 103, no. 2, pp. 529–533, 1981.

[10] E. Litwin-Staszewska, S. Porowski, and A. Filipohenko, "Scattering on short-range potentials in InSb", *Phys. Stat. Solidi (b)*, vol. 48, no. 2, pp. 525–530, 1971.

[11] O. P. Malyk, "Charge carrier mobility in gallium nitride", *Diamond Relat. Mater.*, vol. 23, p. 23, 2012.

[12] Z. M. Fang, K. Y. Ma, D. H. Jaw, R. M. Cohen, and G. B. Stringfellow, "Photoluminescence of InSb, InAs, and InAsSb grown by organometallic vapor phase epitaxy", *J. Appl. Phys.,* vol. 67, 7034, 1990.

[13] Landolt- Bornstein, *Numerical Data and Functional Relationship in Science and Technology*, vol. 17a. Berlin–Heidelberg–New-York: Springer – Verlag, 1982.

[14] S. O. Sari, "Landau transitions at higher gaps in InSb and GaSb", *Solid State Commun.*, vol. 12, pp. 705–708, 1973.

[15] M. E. Straumanis and C. D. Kim, "Lattice Parameters, Thermal Expansion Coefficients, Phase Width, and Perfection of the Structure of GaSb and InSb", *J. Appl. Phys.*, vol. 36, pp. 3822–3828, 1965.

[16] J. R. Drabble and A. J. Brammer, "The third-order elastic constants of indium antimonide", *Proc. Phys. Soc.,* vol. 91, p. 959, 1967.

[17] A. Blacha, H. Presting, and M. Cardona, "Deformation Potentials of $k = 0$ States of Tetrahedral Semiconductors", *Phys. Status Solidi (b)*, vol. 126, pp. 11–36. 1984.

[18] D. L. Rode, "Electron Transport in InSb, InAs, and InP", *Phys. Rev. B*, vol. 3, pp. 3287-–3299, 1971.

[19] K. Aoki, E. Anastassakis, and M. Cardona, "Dependence of Raman frequencies and scattering intensities on pressure in GaSb, InAs, and InSb semiconductors", *Phys. Rev. B*, vol. 30, pp. 681–687, 1984.

[20] G. Arlt and P. Quadflieg, "Piezoelectricity in iii-v compounds with a phenomenological analysis of the piezoelectric effect" *Phys. Status Solidi (b),* vol. 25, p. 323–330, 1968.

[21] O. P. Malyk, "The local inelastic electron–polar optical phonon interaction in mercury telluride", *Computational Materials Science,* vol. 33, no. 1–3, pp. 153–156, 2005.

[22] A. A. Druzhinin, A. P. Dolgolenko, I. P. Ostrovskyi, Yu. M. Khoverko, Iu. R. Kogut "Thermoelectric sensors based on Ge_xSi_{1-x} whiskers", *Journal of Thermoelectricity.*, no. 4, pp. 82–85, 2009.

МІКРОКРИСТАЛИ InSb ДЛЯ СЕНСОРНОЇ ЕЛЕКТРОНІКИ

Анатолій Дружинін, Ігор Островський, Юрій Ховерко, Ігор Хитрук, Кшиштоф Рогацкі

Розглянуто процеси розсіяння електронів на близькодіючому потенціалі, викликаного взаємодією з полярними та неполярними оптичними фононами, п'єзоелектричними та акустичними фононами, іонізованими домішками та центрами статичної деформації в n-InSb з концентрацією дефектів 3×10^{17} $см^{-3}$. У межах точного розв'язку стаціонарного рівняння Больцмана на основі принципу близькодії розраховано температурні залежності рухливості електронів в інтервалі 4,2–500 К. Встановлено добре узгодження теорії та експерименту у дослідженому інтервалі температур. На основі ниткоподібних кристалів InSb розроблено холлівський датчик, дієздатний у широкому температурному інтервалі 4,2–500 К та в області високих магнітних полів (до 10 Тл) з чутливістю ~ 3,5 мВ/Тл.

Anatoliy Druzhynin – D. Sc., professor, Head of the Department of Semiconductor Electronics at the Institute of Telecommunications, Radioelectronics and Electronic Engineering, Lviv Polytechnic National University, Ukraine.

He is also the winner of Ukrainian State Prize in Science and Engineering (2011). The main scientific activities of prof. A. Druzhynin include theoretical and experimental study of strain-induced effects in silicon, germanium and their solid solutions whiskers. Prof. Druzhynin is the Director of the Scientific Research Center "Crystal" at the Department of Semiconductor Electronics and the supervisor of Sensor Electronics Research Laboratory. Prof. Druzhynin has authored more than 500 scientific papers including more than 40 inventor's certificates and patents. Under his supervision, 3 doctors and 11 candidates of technical science have completed their theses.

Ihor Ostrovskyi – D.Sc., professor of the Department of Semiconductor Electronics at the Institute of Telecommunications, Radioelectronics and Electronic Engineering, Lviv Polytechnic National University, Ukraine.

The main scientific activities of prof. I. Ostrovskyi include theoretical and experimental study of strain-induced effects in silicon, germanium and their solid solutions whiskers.

Yuriy Khoverko – Ph. D., senjor researcher, postgradute doctorate student. Department of Semiconductor Electronics of Lviv Polytechnic National University, Ukraine.

Research interests cover physics and technology of semiconductor devices, micro- and nanoelectronic structures and sensor electronics. Research findings have been published in more than 150 scientific papers, and 7 patents have been granted by Ukraine.

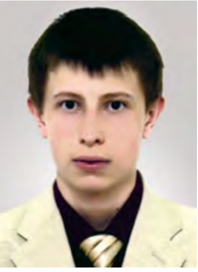

Ihor Khytruk – postgraduate student of the Department of Semiconductor Electronics at the Institute of Telecommunications, Radioelectronics and Electronic Engineering, Lviv Polytechnic National University, Ukraine.

Krzysztof Rogacki – Professor at The Institute of Low Temperature and Structure Research of the Polish Academy of Sciences (ILT&SR) in Wroclaw, where he completed his PhD and habilitation degrees in experimental condensed matter physics in 1990 and 2004, respectively.

He has been the Head of the Superconductivity Department and a Member of the Scientific Council for many years. His current research focuses on classical and high temperature superconductivity including coexistence of magnetism and superconductivity, vortex dynamics, pinning mechanisms and critical currents issues; also on the unconventional effects in high magnetic fields, phase transitions, critical phenomena and low temperature and high vacuum techniques.

Professor Rogacki is the author of more than 100 papers being cited over 1050 times according to the SCI. He has presented more than 90 works at conferences including 15 invited lectures and been the guest speaker at several prestigious scientific institutions such as Jagiellonian University and AGH University in Krakow, Institute of Physics PAS in Warsaw, University of Wroclaw, Wroclaw University of Technology (Poland), University of Tokyo (Japan), ETH Zurich (Switzerland), Argonne National Laboratory (Illinois, USA), and Leipzig University (Germany).